Development and Application of Method to Project Groundwater Infiltration in Sanitary Sewer Systems Affected by Sea Level Rise

By Adrienne Carmen Fung

Submitted to the University of Hawai‘i at Manoa
Department of Civil and Environmental Engineering

In Partial Fulfillment of the Requirements for the
Degree of Master of Science in Civil Engineering
May 2019

Committee Members:

Chair: Roger Babcock, Department of Civil and Environmental Engineering

Daniele Spirandelli, Department of Urban and Regional Planning

Tao Yan, Department of Civil and Environmental Engineering

Abstract:

Coastal sanitary sewer networks are increasingly at risk of groundwater infiltration (GWI) into pipes due to sea level rise (SLR). As sea level increases, so does the groundwater table, causing sanitary sewer pipes to become submerged. If structural defects or deterioration, such as cracks, are present, submerged pipes will be subject to GWI. Therefore, there is a strong need for GWI projections as SLR persists. While previous methods relied on specialized modeling expertise or general infiltration parameters, this thesis describes a user-friendly procedure based on a two-dimensional (2D) GWI model with explicit parameters that better visualize circumstances of the network. These parameters include hydraulic head, which is proportional to SLR, and pipe defect size, which is used to prioritize pipes for improvement. Using flow monitoring data, the 2D GWI model was calibrated for the network in three-meter-pipe intervals. Data analysis and calibration were performed using Microsoft Excel and U.S. Environmental Protection Agency's Sanitary Sewer Overflow Analysis and Planning Toolbox.

Pipes that are currently submerged and pipes that will be eventually submerged were investigated individually. Firstly, for pipes that are currently under the groundwater table and subject to GWI, the flow meter measurement provides a sum of GWI in the upstream pipes. To determine the flow in *each* of the three-meter pipe segments, two methods of calibration were explored. Following calibration, future GWI was projected by increasing hydraulic head depending on the level of SLR. Secondly, different methods of GWI projections were tested for pipes that will be eventually submerged due to future SLR. These methods included a severity matrix of varying defect sizes and lengths of pipes with defects, a mathematical relationship based on previous calibration results, and an effective defect size that is representative of the porosity of a given sewer area. In conclusion, a flow chart is presented with GWI projection methods that are recommended based on availability of flow monitoring data or system knowledge.

Advisor: Roger Babcock
Title: Professor

Acknowledgments:

- I am extremely grateful to have had the opportunity to work with Dr. Babcock. I always looked forward to our brainstorming sessions, and his encouragement and patience are very much appreciated.

- Thank you to Dr. Spirandelli for welcoming me to this project when it was first part of a project that was sponsored by the University of Hawai‘i Sea Grant Program. Through her, I have also met other professionals working with sea level rise adaptation. Thank you also to Dr. Spirandelli for being on my thesis committee and for her very helpful insights.

- I am fortunate to have Dr. Yan on my thesis committee as well. I am very thankful for his constructive feedback and support throughout my studies.

- The Department of Civil and Environmental Engineering helped me to grow as a learner and also as a member of my community. I met many wonderful friends here and am grateful for their support.

- Thank you from the bottom of my heart to my family and friends for their continuous love.

Table of Contents

1.0 INTRODUCTION

Sea level has been historically rising due to ocean warming and expansion and glaciers and polar ice caps melting and losing ice [1]. This phenomenon has, and will continue to, negatively impact the quality of life in natural and human systems by increasing erosion, submergence and flooding of coastal land, loss of habitats and evacuation of homes, and saltwater intrusion and aquifer and soil contamination [2]. Recent sea level rise (SLR) projections were updated in 2017 by the National Oceanic and Atmospheric Administration (NOAA), ranging from a 0.3-meter (m) to 2.5-m rise in the global mean sea level by 2100 in the lower-bound and extreme upper-bound scenarios, respectively [3]. Figure 1 depicts the projections of varying degrees of six scenarios (starting from the lowest line on the right: low, intermediate-low, intermediate, intermediate-high, high, and extreme) relative to data collected from 1800 to 2015 (black and magenta lines). More recently, however, the rate of SLR in the past few decades has been found to be accelerating at approximately 0.08 millimeters (mm) per year each year, rather than as previously assumed, steadily increasing at about 3 mm per year [4]. The 2017 NOAA projections, and earlier ones, were based on a constant SLR increase; therefore, the new finding of accelerated SLR indicates that those projections may be underestimates. This raises the concern of SLR and need to act, especially at coastal areas, which are most affected.

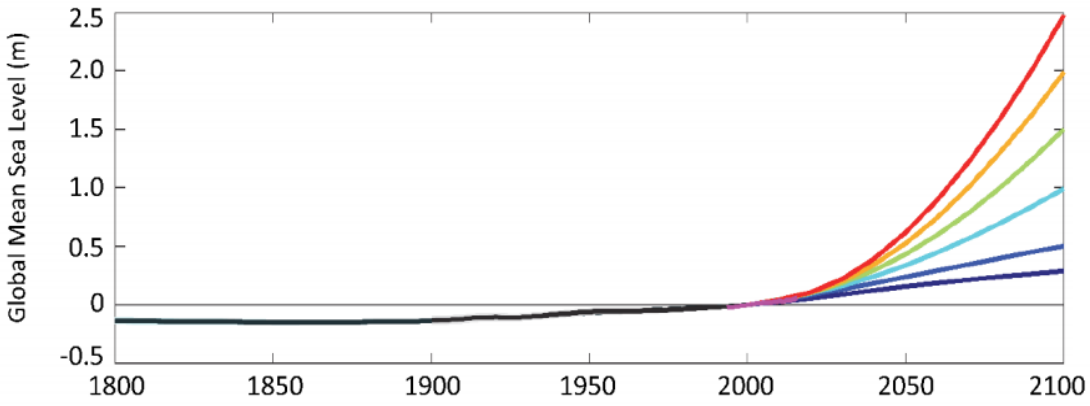

Figure 1. NOAA Predictions for Global Mean Sea Level Rise Scenarios Relative to Years 1800 to 2015 [3]

The impact of SLR on coastal regions has been well understood. In coastal communities, the groundwater table meets the sea surface at an interface and as the sea level rises, the groundwater elevation also rises, as depicted in Figure 2 [5] [6] [7] [8] [9] [10] [11] [12] [13] [14]. Groundwater impacts from SLR are substantial, occurring farther inland than surface water effects or causing flood volumes that rival those caused solely by surface flooding [7] [14] [10]. Because of these impacts, infrastructure must be properly protected from flooding and other damages.

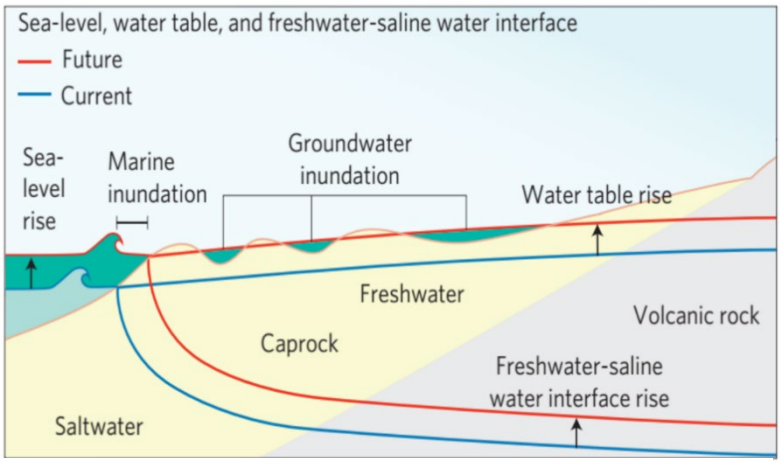

Figure 2. Impacts of SLR on Groundwater Table [5]

Examples of vital infrastructure are wastewater assets and facilities, which serve millions of users each day. In wastewater infrastructure, sewer pipes receive a constant amount of groundwater infiltration (GWI). This infiltration occurs through structural defects caused by leaks at joints, external pipe deterioration due to pipe materials and soil chemical composition, internal pipe deterioration due to sulfide attack, stresses from soil movement (soil shrink and swell), and traffic loading [15]. In coastal systems, some sewer pipes are currently located below the groundwater table, and as sea level continues to increase, additional pipes will fall below this table. This will in turn raise the amount of groundwater that will infiltrate sewer pipes. While a practical design criterion is to assume 10 to 25 percent (%) of domestic sanitary sewer flow as

GWI [16], this value underestimates the actual amount of GWI that has been observed [17]. Moreover, this percent will continue to increase due to SLR.

Increases in GWI contribute to additional hydraulic load in the sanitary sewer system, leading to sewage dilution and decreased treatment efficiency, higher operation and treatment costs to account for increased load, and more incidents of sanitary sewer overflows (SSOs), which harm human health, infrastructure and economic investments, and the environment [18] [19]. To mitigate or prevent these incidents, planning and management tools will help project increases in GWI and prioritize portions of the sanitary sewer system for rehabilitation. Holistic water management models have been developed to address water pathways in urban water infrastructure [20]. These incorporate multiple aspects of the urban water cycle, including GWI, groundwater exfiltration, land use data, surface runoff, drainage systems, and indoor and outdoor water use. However, these models focus on the interaction between each of these components, rather than the individual calculations of each contributor. Therefore, users typically must input each separate component, or at most, a limited number of standard parameters or assumptions that are then used to estimate the component. Since these usually stem from typical criteria or general observations, users would benefit from a more rigorous and accurate determination of the individual parameters, especially ones not directly measured, like GWI.

To quantify GWI, researchers have developed various methods, including GWI potential maps [21], fluid mechanics models with infiltration or permeability coefficients [17], and commercial software models [22] [23] [24] [25]. However, reliable methods for planning and prevention remain inaccessible due to limited resources in funding and trained modelling specialists. Furthermore, most models do not use explicit variables to characterize wastewater systems, but rather use a general infiltration or permeability coefficient.

A promising model is a recently developed two-dimensional (2D) model to estimate GWI into sanitary sewer pipes [26]. This model assumes a line defect running along the pipe wall and uses commonly available data: surrounding soil hydraulic conductivity, groundwater elevation, pipe invert elevation, sewer pipe radius, defect position, and defect size. The advantages of this 2D model include 1) using individual variables for major contributing factors of surrounding soil hydraulic conductivity and pipe defect, size, and location; 2) calculating GWI per pipe segment at a higher resolution compared to evaluating the network as a single entity; 3) establishing a direct relationship between SLR and GWI; and 4) removing the need for complicated or expensive software and highly specialized modeling expertise.

The primary goal of this thesis is to develop a procedure that is both reliable and user-friendly. To test the procedure, flow data was obtained for a coastal sanitary sewer network. The data was assessed for usability and GWI was quantified using the U.S. Environmental Protection Agency's (EPA) Sanitary Sewer Overflow Analysis and Planning (SSOAP) Toolbox software[1]. Afterwards, flow data was used with Microsoft® Excel Solver[2] to calibrate the 2D GWI model. With a calibrated model, different methods were investigated for projecting increases in GWI due to SLR. The projections were evaluated, and the recommended methods are presented in a flowchart for selecting an appropriate procedure for projecting GWI.

2.0 METHOD

2.1 Collection of Flow Monitoring Data

The study area is a sanitary sewer network located approximately 200 to 400 meters (m) from the coast. System data were allowed for use provided that the location and wastewater

[1] Provided free of charge at https://www.epa.gov/water-research/sanitary-sewer-overflow-analysis-and-planning-ssoap-toolbox#downloads.

[2] The Solver Add-In is a Microsoft Office Excel add-in program that is readily available after installing Microsoft Excel.

agency remain anonymous. This site was selected as a representative of coastal areas facing SLR threats to their sanitary sewer networks. The study area, like many coastal areas, is extremely tied to the behavior and fate of the sea; for example, construction projects working below ground either require dewatering or are scheduled to occur during times of low tide. Therefore, adaptation to SLR is of utmost importance.

The flow and rainfall data are from a monitoring period of 10 consecutive weeks. Ten flow meters and two rain gauges were installed throughout nearly 9,800 m of sanitary sewer lines. The flow meters logged level and velocity readings every five minutes, and the rain gauges recorded rainfall data every five minutes.

The flow meters utilized continuous wave Doppler technology to measure content level and velocity [27]. A sensor transmitted a continuous ultrasonic wave and then measured the frequency shift of returned echoes reflected by air bubbles or particles in the flow. This frequency shift was used to derive a mean velocity. An integrated differential pressure transducer measured level. Rain gauges were needed to determine dry weather periods, which is important for estimating GWI, which is described in more detail later.

2.2 Determining Groundwater Infiltration

Using the velocity and level monitoring data, volumetric flow was calculated using Darcy's Law. An expression for the flow area (A_x) was derived first. The flow meter records the depth of the content, which fills the pipe up to the blue line, as shown in Figure 3. The angle θ_1 is half the angle θ that is formed by the circular sector. To determine the cross-sectional area of the flow, the area of triangle ABC is subtracted from the circular sector θ: $A_x = A_\theta - A_{ABC}$.

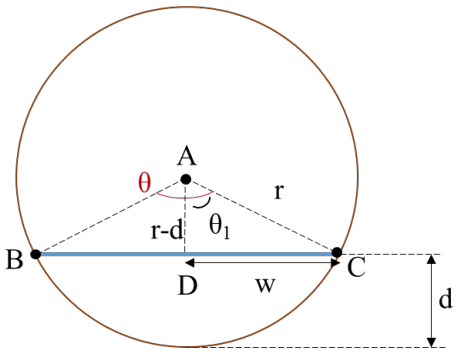

Figure 3. Schematic of Pipe Cross-Section

To determine A_θ, triangle ACD with height radius r less flow depth d, and width w is used to determine θ_1:

$$\theta_1 = \cos^{-1}\left(\frac{r-d}{r}\right) \qquad \text{Equation 1}$$

Given that $\theta = 2*\theta_1$, the area of the circular sector can then be calculated:

$$A_\theta = (\pi r^2)\left(\frac{\theta}{2\pi}\right) = \frac{1}{2}r^2\theta = \frac{1}{2}r^2\left(2 * \cos^{-1}\left(\frac{r-d}{r}\right)\right) = r^2\cos^{-1}\left(\frac{r-d}{r}\right) \qquad \text{Equation 2}$$

To determine the area of ABC, the Pythagorean Theorem is used to calculate the base, 2*w:

$$2w = 2\sqrt{r^2-(r-d)^2} \qquad \text{Equation 3}$$

Using the formula for the area of a triangle, the area of ABC is calculated to be:

$$A_{ABC} = \frac{1}{2}\left(2\sqrt{r^2-(r-d)^2}\right)(r-d) = (r-d)\sqrt{r^2-(r-d)^2} \qquad \text{Equation 4}$$

Finally, the cross-sectional area A_x is:

$$A_x = r^2\cos^{-1}\left(\frac{r-d}{r}\right) - (r-d)\sqrt{r^2-(r-d)^2} = r^2\cos^{-1}\left(1-\frac{d}{r}\right) - (r-d)\sqrt{2rd-d^2} \qquad \text{Equation 5}$$

To calculate flow rate Q, A_x is multiplied with velocity v:

$$Q = A_x v = vr^2 \cos^{-1}\left(1 - \frac{d}{r}\right) + (vd - vr)\sqrt{2rd - d^2} \qquad \text{Equation 6}$$

Next, the flow data was assessed for quality and usability depending on sewer performance. For example, data from a meter installed in a manhole subject to frequent surcharging could not be used for the model. Under circumstances of typical gravity flow behavior, flow volume increases with level. During surcharging, however, the accuracy of flow measurements is affected because flow within the pipe may shift from gravity flow to pressure flow, flow volume may have spilled out and left the system, or backups are causing a low velocity to be measured. Data exhibiting "typical" sanitary sewer performance is also needed for accurate model calibration. These data exhibit diurnal flows, which rise during the day and fall at the night. Figure 4 is an average dry weather flow (DWF) hydrograph for weekday and weekend flow. As observed, flow starts increasing at the beginning of the day due to increased water usage. The water usage mildly fluctuates around an average value throughout the day, and goes up again slightly starting in the early evening. The flow decreases once more later in the night. For usability and model calibration, flow meter FM-5 was selected, which measured about 1,445 m of upstream sewer line.

SSOAP Toolbox was then used to estimate GWI of the upstream pipes measured by FM-5 ($Q_{Actual,\ All\ Pipes}$). This value, $Q_{Actual,\ All\ Pipes}$, is based on two criteria: 1) nighttime minimum flow and 2) dry weather flow [28] [29]. Base wastewater flow is minimal at night, as is rainfall-derived inflow and infiltration during dry weather; therefore, on a dry weather day at nighttime, the primary flow should be GWI, as approximated by the orange bar in Figure 4. Days were selected as DWF days if their rainfall did not exceed a maximum amount of 2.54 mm over the

preceding three days. For this study area, eight DWF days met the criteria, and a $Q_{Actual,\ All\ Pipes}$ was determined for each day using hydrograph analysis with SSOAP Toolbox.

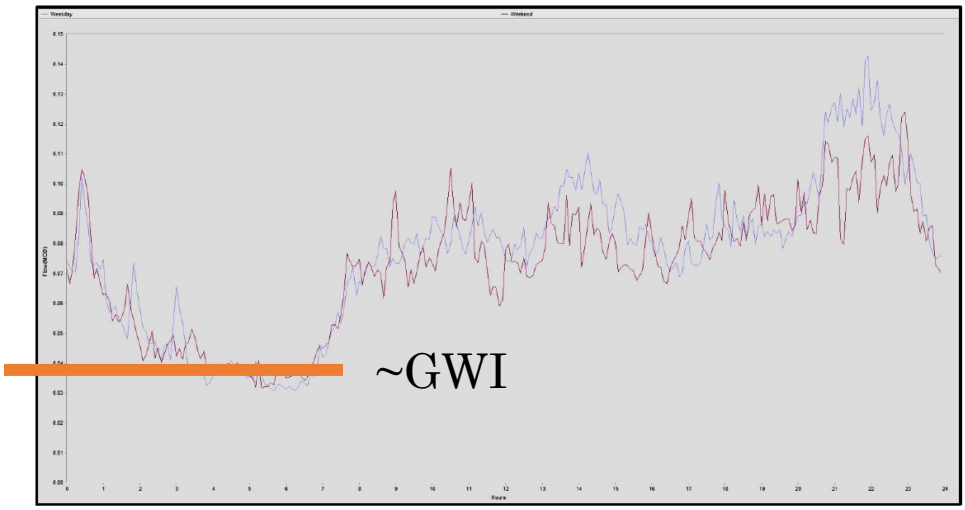

Figure 4. Example Hydrograph and Estimate of GWI

2.21 Validation of Dry Weather Flow Days

Statistical analysis of cross-correlation was used to compare the different time-series among DWF Days 1-8 at various lags. The results allowed us to evaluate the strength between two series and determine the lag that maximized the correlation between them. The cross-correlation was calculated between flows on DWF Day 1 and each of the other DWF days. Table 1 lists the highest cross-correlation r_τ and the lag τ at which they occur. Because the corresponding periods ($\Delta t^*\tau$) are near the time origin for each of these r_τ, the correlations are maximized close to the zero lag position, which confirms that the data sets are most similar when their time axes directly overlap.

Cross-correlations can also be tested in two-sided t-tests with the null hypothesis that the two compared series statistically have the same means at the 95% confidence level. Since n is large, the critical t is 1.96, based on the normal distribution. If the observed t statistic exceeds the critical t value, then the null hypothesis is rejected, and it is concluded that the two series are not the same. As shown in Table 1, each observed t statistic is less than the critical t value.

Therefore, the null hypothesis cannot be rejected, and it is concluded that the samples have the same statistical means at the 95% confidence level.

Date	Highest Cross-Correlation			Significance at 95% Level of Confidence	
	Lag τ	Cross-Correlation r_τ	Period in Minutes	Observed t value	Significant?
11/30/14	1	0.00005701	5	0.00096	No
12/1/14	1	0.0001975	5	0.0033	No
12/2/14	0	0.0001157	0	0.0020	No
12/6/14	0	0.00005764	0	0.00097	No
12/7/14	8	0.0001056	40	0.0018	No
12/8/14	0	0.0001482	0	0.0025	No
12/9/14	-1	0.0001052	5	0.0018	No

Table 1. Summary of Highest Cross-Correlations with 11/27/14 Data and their Significance

2.22 Potential Groundwater Infiltration

The GWI ($Q_{Actual,\ All\ Pipes}$) determined by SSOAP Toolbox is the sum of GWI in upstream pipes. Therefore, another step was taken to calculate flow in *each* pipe segment. The pipes were divided into 3-m segments, and a potential GWI (PGWI) parameter was determined for each section. PGWI is the GWI that could possibly occur, assuming complete saturation in surrounding soil. To calculate PGWI, two approaches were used, both assuming pipes with equal defect sizes. The first is a linear representation of PGWI and assumes a rectangular volume of groundwater surrounding the pipe. To determine the PGWI in this setup, the volume of the pipe segment $\left(\pi\left(\frac{d}{2}\right)^2 l\right)$ was first subtracted from the saturated volume of groundwater $\left(\left(h+\frac{d}{2}\right)dl\right)$, given a pipe with diameter d and length l (Figure 5). The PGWI expression also

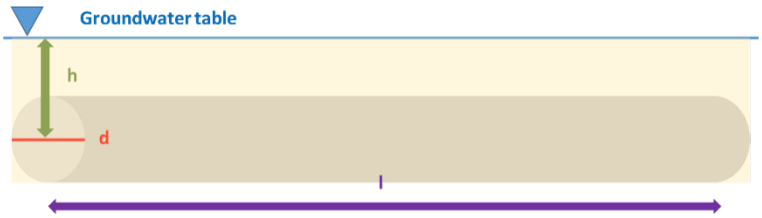

Figure 5. Diagram of Linear PGWI Calculation

has a factor of hydraulic conductivity k, since this affects the degree of GWI. For example, two identical pipe segments could have the same defect sizes and hydraulic heads, but the pipe segment in soil with higher hydraulic conductivity would be expected to have more GWI. The resulting equation is a function of pipe length and diameter, hydraulic head, and surrounding soil hydraulic conductivity:

$$PGWI = lk\left(hd + \left(\frac{2-\pi}{4}d^2\right)\right) \qquad \text{Equation 7}$$

A PGWI is calculated for each pipe section, $PGWI_{\text{Pipe Segment}}$, and these are summed up to obtain a total as $PGWI_{\text{All Pipes}}$. A proportion can then be set up as the following:

$$\frac{PGWI_{Pipe\ Segment}}{PGWI_{All\ Pipes}} = \frac{Q_{Actual,\ Pipe\ Segment}}{Q_{Actual,\ All\ Pipes}} \qquad \text{Equation 8}$$

This will allow for the GWI of an individual pipe segment ($Q_{\text{Actual, Pipe Segment}}$) to be calculated. The second way that PGWI was calculated was with the 2D model, which is described in more detail in the following section. This also resulted in a $PGWI_{\text{Pipe Segment}}$ and $PGWI_{\text{All Pipes}}$ that were used with Equation 8 to determine $Q_{\text{Acual, Pipe Segment}}$.

2.3 Calibration of 2D GWI Model

The 2D model is a function of commonly available pipe and soil characteristics and allows for the calculation of GWI [26]. The model assumes the surrounding soil is homogeneous and isotropic with a constant hydraulic conductivity, and the groundwater table is horizontal. Darcy's law and mass conservation are combined to represent 2D flow around a defect, resulting in a Laplace equation of the hydraulic head, which is a sum of the pressure and elevation heads. Boundary conditions are set at the groundwater surface, defect, and the pipe wall on the other side of the defect, but because of their complexity, an approximate solution is considered more practical and logical. This is achieved using an equivalent circumference method and Mobius

transformation. The process transforms the line defect into a circle with a circumference equal to the length of the line defect. The circle is then mapped into the complex plane using the Mobius transformation, preserving the Laplace equation. The boundary conditions translated into polar coordinates, and solving the Laplace equation results in the following:

$$Q = 2\pi k\left(h\frac{1-\lambda'^2}{1+\lambda'^2} - p\right)\ln^{-1}\left(\frac{2\pi}{\beta}\left(\frac{h}{r} - sin\alpha\right)\left(1 + \sqrt{1 - \left(\frac{\beta}{2\pi\left(\frac{h}{r} - sin\alpha\right)}\right)^2}\right)\right)$$

$$\text{With } \lambda' = \frac{2\pi}{\beta}\left(\frac{h}{r} - sin\alpha\right) - \sqrt{\left(\frac{2\pi}{\beta}\left(\frac{h}{r} - sin\alpha\right)\right)^2 - 1} \qquad \text{Equation 9}$$

The variables for surrounding soil hydraulic conductivity k, hydraulic head h, pipe radius r are generally available for sewer lines, and assumptions can be made for pressure head p and pipe defect location α. Defect size β is the target parameter for calibration.

A geographic information system (GIS) asset management database of the sanitary sewer network included information such as pipe material, length, radius, installation date, slope, and invert elevations. The pipe radii from this database were used for the model. These values ranged from 7.62 to 12.7 centimeters (cm).

To ascertain the study area's hydraulic conductivity, the GIS map of pipe locations was first overlaid with a map of soils in the study area. After determining the soil type that was surrounding each 3-m pipe segment, a U.S. Department of Agriculture (USDA) and Natural Resources Conservation Service (NRCS) Custom Soil Resource Report was used to identify the hydraulic conductivity. The soil hydraulic conductivity of this area is high, ranging from 1.4E-5 to 1.4E-4 m per second (m/s). For each soil, a range of hydraulic conductivities is provided by

the soil report; for a conservative approach, the lower limit was initially used for model calibration.

Afterwards, hydraulic head was calculated for each pipe segment by subtracting the mean pipe invert and radius from the groundwater elevation. Pipe invert elevations were provided in the GIS database, and groundwater elevations were interpolated based on daily groundwater elevation measurements from a U.S. Geological Survey monitoring well. The groundwater table is shallow in the study area, about 0.3 to 0.5 m above mean sea level.

Structural analysis tests have demonstrated that line defects are usually generated at the crown, invert, and springlines: $\alpha = \pi/2$, $3\pi/2$, 0 and π, respectively [30] [31]. When the defect is above the pipe content level ($p = 0$), then a crown defect ($\alpha = \pi/2$) leads to the largest rates of GWI [26]. To use a conservative approach, p was assumed as 0, and α was assumed as $\pi/2$.

With these model input parameters determined, model calibration was performed to obtain calibrated defect sizes of β. For each pipe segment, Microsoft® Excel Solver used an initial value of β and calculated a $Q_{Model,\ Pipe\ Segment}$, which was compared to the $Q_{Actual,\ Pipe\ Segment}$. By coding the process into Visual Basic for Applications (VBA), this process was iterated until $Q_{Model,\ Pipe\ Segment}$ was equal to $Q_{Actual,\ Pipe\ Segment}$.

Once calibration of the various β was completed, the groundwater elevation was increased by a projected amount of sea level gain and a new, projected $Q_{Model,\ Pipe\ Segment}$ was calculated with Equation 9. Although SLR-induced groundwater rise is not spatially uniform due to heterogeneous depositional environmental and hydraulic properties of geologic materials [32], the study area is in such close proximity to the coastline that spatial effects are negligible and a 1:1 ratio of groundwater rise to SLR was used. Although NOAA recommends that the

extreme scenario be used to plan for infrastructure when there is low tolerance for risk [33], different sea level increases were evaluated to generate a range of potential projections.

2.4 Procedure Limitations

GWI was estimated to be 100% of the nighttime minimum flow generated by the SSOAP Toolbox software. In reality, 100% cannot be attained because base wastewater flow is never at zero, even at night. Usually, the GWI fraction of the nighttime minimum is assumed to be 80 to 90 percent in predominantly residential areas, and as low as 50 percent in college towns, business districts, and industrial areas [29]. Therefore, knowledge of the demographics of an area is an important input to refining the GWI that is used in calibration.

In modeling, assumptions and results should be validated by experimental or site-specific field tests. Even in the best-case scenario where field tests can be performed, a single site test may still not be representative of the overall area. In this study, flow meters were staggered throughout the sanitary sewer lines to maintain a sufficient level of accuracy for subsections of the network. When selecting FM-5 for analysis, its associated upstream portion was carefully isolated from the rest of the network. Therefore, FM-5 is representative of the potential of the overall procedure and its repeatability for other flow meters.

Due to everchanging field conditions, models are simplified representations of current situations. Projections, therefore, are extensions of the present. It is recognized that models will have some deviations from reality, but these are difficult, if even possible, to measure accurately. One example of a deviation is hydraulic head, which is typically a straightforward calculation based on groundwater and pipe invert elevations. However, significantly high hydraulic head could lead to potholes in the vicinity of the leak area, flushing of soil particles in the vicinity of a leak, and enlargement of the leak size that was previously assumed [25]. It would be no small feat to identify where this phenomenon would occur without dedicating more resources to

extensive investigation and monitoring. Flow data was collected for ten weeks, which is reflective of the amount of time and financial resources that can usually be dedicated by a municipality for a flow monitoring study.

Other factors that play a role but were not explicitly represented in the model include ocean tides or seasonal recharge rates or fluctuations in nearby rivers or bodies of water [6] [17] [16]. While the study area is located near the shore and subject to tidal influences, the mean groundwater elevations were used as model inputs. The study area has both a wet and dry season, and although the study took place in the wet season, selection criteria were used to identify and isolate days of dry weather flow (DWF). There were no nearby freshwater bodies, so the model results are not affected by excluding contributions from this source.

3.0 RESULTS: MODEL CALIBRATION AND APPLICATION TO SLR IMPACTS

3.1 Scenarios C-X: Current Effect of SLR on Submerged Pipes

In the study area of approximately 1,445 m of sewer line in the study area, roughly 6% are located below the groundwater table, and therefore, potentially affected by GWI. Based on monitoring data and SSOAP Toolbox analysis, the mean GWI was measured to be 132 cubic meters per day (m^3d^{-1}) with a standard deviation of 27.3 m^3d^{-1} (Table 2). The difference among the GWI may be due to tidal influences. The model was calibrated using the two different methods of calculating PGWI (linear and 2D model), and the resulting GWI projections were compared.

DWF Day	GWI (m^3d^{-1})
1	156.3
2	80.6
3	154.8
4	138.5
5	145.0
6	142.7

DWF Day	GWI (m^3d^{-1})
7	99.2
8	140.4
Mean	**132.2**
Standard Deviation	**27.3**

Table 2. Groundwater Infiltration for each Dry Weather Flow Day

3.11 Scenario C-L: Linear Relationship to Calculate PGWI

Beginning with the linear expression for GWI, the early iterations of calibrating defect size β resulted in unrealistic β values that were too large. For example, a 30.5-cm radius pipe needed a β of nearly 7 radians to calculate a $Q_{Model,\ Pipe\ Segment}$ that would be equal to its associated $Q_{Actual,\ Pipe\ Segment}$. This is not physically possible, as a β of 7 radians is a 213-cm-long arc defect, which exceeds the pipe circumference. Additionally, the model is recommended for small defect sizes, such as a β of π/18 radians, or 52 mm for a 30.5-cm radius pipe.

While the other variables are based on physical pipe characteristics or are less spatially varying, such as pipe radius and groundwater elevation, hydraulic conductivity k was further investigated. This variable is relatively ambiguous due to limited comprehensive soil studies in most areas. Since the lower bound of the USDA and NRCS Custom Soil Resource Report was used in the initial calibration, the upper bound was used in another round of calibration. With these higher k values, the β values were more reasonable values and within the recommended range of the model. It is recommended that a soil test be performed in the vicinities of the sewer pipes. This should be done outside the backfill area, as backfill material is of such low density that it will not be a controlling factor in GWI. Using these updated β values in the calibrated model, SLR effects were applied in various ranges of 0.30 to 2.7 m (Table 3). For a NOAA projection of 0.3 m in a low risk scenario, the mean GWI is 217 cubic meters per day (m^3d^{-1}) by the year 2100. This projection increases by 77% in an intermediate risk scenario of 0.9 m, and by 220% in a high risk scenario of 2.1 m.

SLR (m)	0.3	0.6	0.9	1.2	1.5	1.8	2.1	2.4	2.7
DWF Day	**GWI (m^3d^{-1})**								
1	253	348	439	528	615	701	784	867	949
2	250	344	434	522	608	692	775	857	937
3	144	206	266	325	383	440	496	552	608
4	228	315	400	482	562	641	718	795	870
5	232	320	404	486	566	644	721	797	871
6	229	316	400	481	560	638	714	790	864
7	172	243	312	379	444	509	572	635	697
8	225	310	392	471	549	625	699	773	845
Mean	**217**	**300**	**381**	**459**	**536**	**611**	**685**	**758**	**830**

Table 3. Use of Linear PGWI Relationship to Project Groundwater Infiltration for Currently Affected Pipes

3.12 Scenario C-M: 2D Model to Calculate PGWI

An artifact of using the linear method to calculate PGWI is the increase in calibrated β with hydraulic head h. This was due to the linear relationship between PGWI and h. However, a pipe at lower groundwater elevation may not necessarily have a smaller crack size. Defects also depend on a pipe's age, material, and other physical features. Therefore, another method for determining PGWI is to use the 2D GWI model (Equation 9). In the model, GWI and h are not linearly related because of the inverse natural logarithm. (When using the model to calculate the PGWI, and in subsequent β calibration, the updated hydraulic conductivities from the earlier calibration (from Section 3.11) were retained.)

Since the model is a function of β, this raises the question of what β to use in the calculation of PGWI. Initial β values for calibration were selected from a range of π/18 to π/90, but the resulting calibrated βs varied minimally for a given DWF day (Figure 6). For example, DWF Day 6 has calibrated βs of 0.295, 0.303, and 0.312 for initial βs of π/18, π/32, and π/90, respectively. This is likely because a single initial β was used to calculate PGWI, and so the resulting β values vary less. There is more variation across the different DWF days, so more information about the sanitary sewer system, such as tidal effects on it and nighttime non-GWI

contributions, may be helpful. Nevertheless, a grand mean (orange line in Figure 6) of the calibrated βs, 0.197 radians, was identified as an "effective β" of the system. This effective β is not necessarily thought of as an actual crack size, but as a measure of the overall porosity of the sanitary sewer system. It was used in the calibrated model to generate projections (Table 4). In a low risk scenario of a 0.3 m rise in sea level, by the year 2100, the projected mean GWI is 227 m^3d^{-1}. GWI increases by 77% in an intermediate risk scenario of 0.9 m SLR, and by 219% in a high risk scenario of 2.1 m SLR.

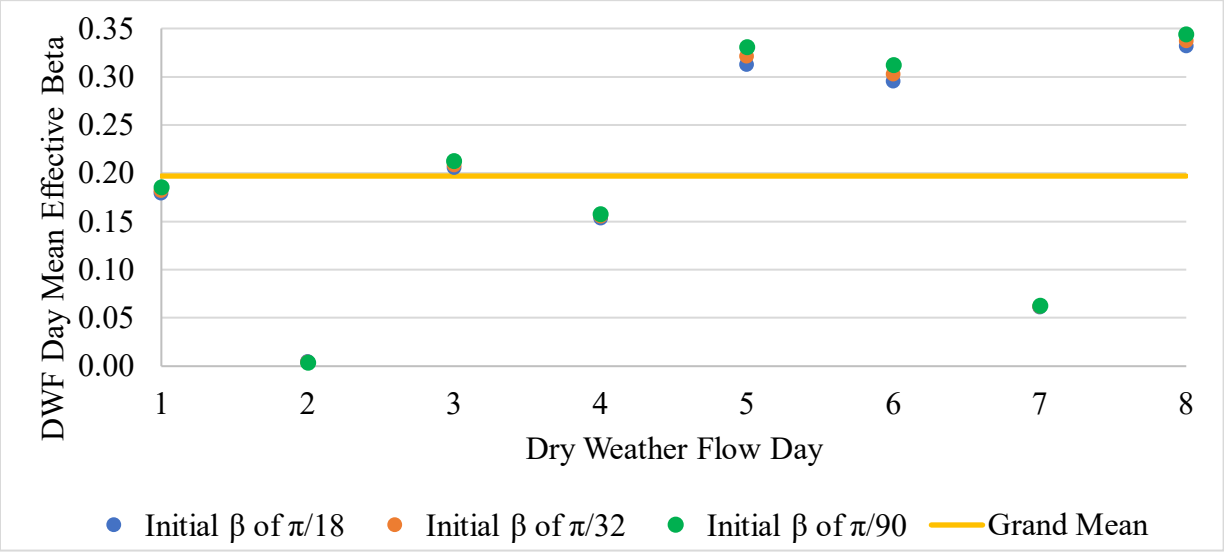

Figure 6. Effects of Initial β on the Final Effective β

SLR (m)	0.3	0.6	0.9	1.2	1.5	1.8	2.1	2.4	2.7
DWF Day	**GWI (m^3d^{-1})**								
1	255	353	447	538	628	715	802	887	971
2	253	351	445	537	626	714	800	885	969
3	246	340	432	521	607	692	776	859	940
4	236	328	417	503	587	670	751	831	909
5	208	291	372	449	526	600	674	746	817
6	208	291	372	449	526	600	674	746	817
7	207	291	371	449	525	600	673	745	817
8	200	281	358	433	507	579	650	719	788
Mean	**227**	**316**	**402**	**485**	**566**	**646**	**725**	**802**	**879**

Table 4. Use of 2D Model to Calculate PGWI and Project Groundwater Infiltration for Currently Affected Pipes

3.2 Scenarios F-X: Future Effect of SLR on Pipes

As sea level increases, additional pipes will become submerged and have higher chances of undergoing GWI (Figure 7). Because these are future events with no GWI data in the present, scenarios were developed and assessed for their projections of SLR impacts on these pipes:

1. Severity matrix (Scenario F-SM)
2. Mathematical relationship between defect size and hydraulic head (Scenario F-βh)
3. Effective defect size (Scenario F-Eβ)

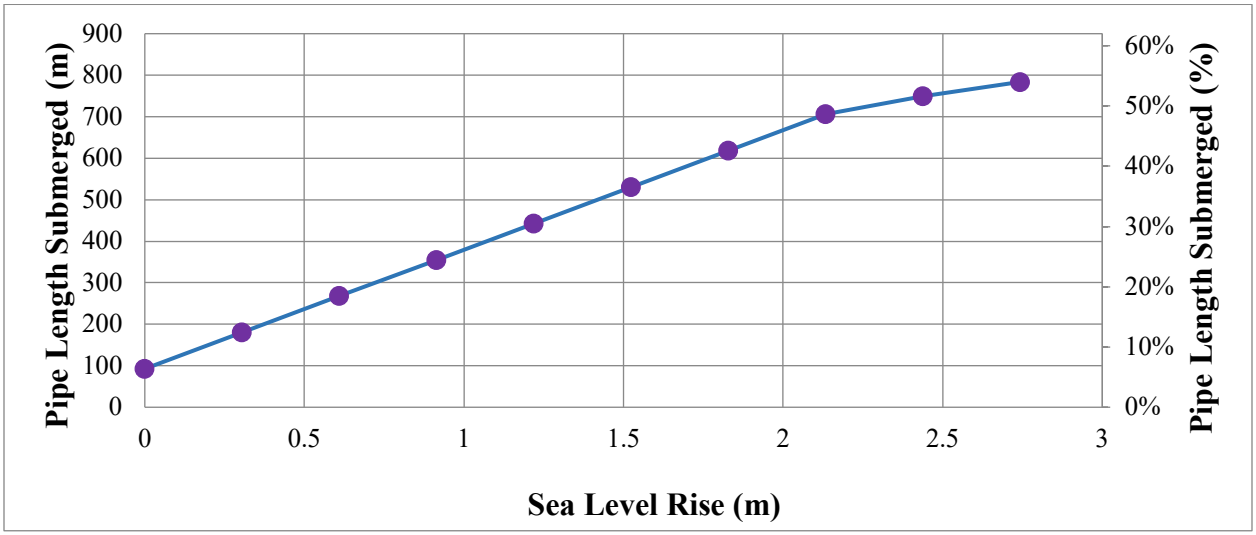

Figure 7. Length of Sewer Line Affected as Sea Level Increases

3.21 Scenario F-SM: Severity Matrix

In the first method, a severity matrix was developed with 12 cases of varying degrees of defect size and percent of sewer line length that is affected by GWI, as conveyed in Table 5. Defect size is one of the severity matrix variables, as it strongly pertains to the state of the pipe. Moving vertically down the cases in the matrix, the defect size increases from $\pi/90$ to $\pi/18$. Moving horizontally across the cases, the defect size remains the same, and the percent affected increases from 5% to 100%. This percent parameter controls the length of pipes affected by GWI because while a pipe segment is submerged by groundwater, it may not be subjected to

GWI if it does not contain open defects. Therefore, the varying combinations of defect size and percent affected can be used to project GWI for different parts of the sanitary sewer system. Based on system knowledge, rehabilitated lines could be represented by cases with smaller defect sizes or lower percent affected. Cases with larger defect sizes or higher percent affected could be used for projections of worsening lines. In the study area, each case was applied in order to analyze the full range of the severity matrix.

	Increasing % of Sewer Line Length Affected →			
← Increasing Defect Size	**Case 1** $\beta = \pi/90 \approx 0.035$ % affected = 5%	**Case 4** $\beta = \pi/90 \approx 0.035$ % affected = 30%	**Case 7** $\beta = \pi/90 \approx 0.035$ % affected = 75%	**Case 10** $\beta = \pi/90 \approx 0.035$ % affected = 100%
	Case 2 $\beta = \pi/30 \approx 0.10$ % affected = 5%	**Case 5** $\beta = \pi/30 \approx 0.10$ % affected = 30%	**Case 8** $\beta = \pi/30 \approx 0.10$ % affected = 75%	**Case 11** $\beta = \pi/30 \approx 0.10$ % affected = 100%
	Case 3 $\beta = \pi/18 \approx 0.17$ % affected = 5%	**Case 6** $\beta = \pi/18 \approx 0.17$ % affected = 30%	**Case 9** $\beta = \pi/18 \approx 0.17$ % affected = 75%	**Case 12** $\beta = \pi/18 \approx 0.17$ % affected = 100%

Table 5. Cases for Pipes Newly Submerged due to SLR

The results show that there is a larger effect of the percentage of pipes affected, compared to the defect size (Figure 8). For a SLR of 0.3 m, Case 1 projects GWI 61 m^3/d for 5% of newly submerged pipes with a defect size of $\pi/90$, while Cases 4, 7, and 10 project GWI of 626 m^3/d, 1,567 m^3/d, and 2,090 m^3/d, respectively, for increasing percentages of affected pipes with the same defect size. Compared to Cases 2 and 3 with increasing defect sizes but the same percent affected, GWI rates are 123 m^3/d and 134 m^3/d, respectively. Therefore, there is a smaller difference among Cases 1, 2, and 3 than among Cases 1, 4, 7, and 10. Using the SLR predictions from NOAA or other sources, this figure can be used to project increases in GWI.

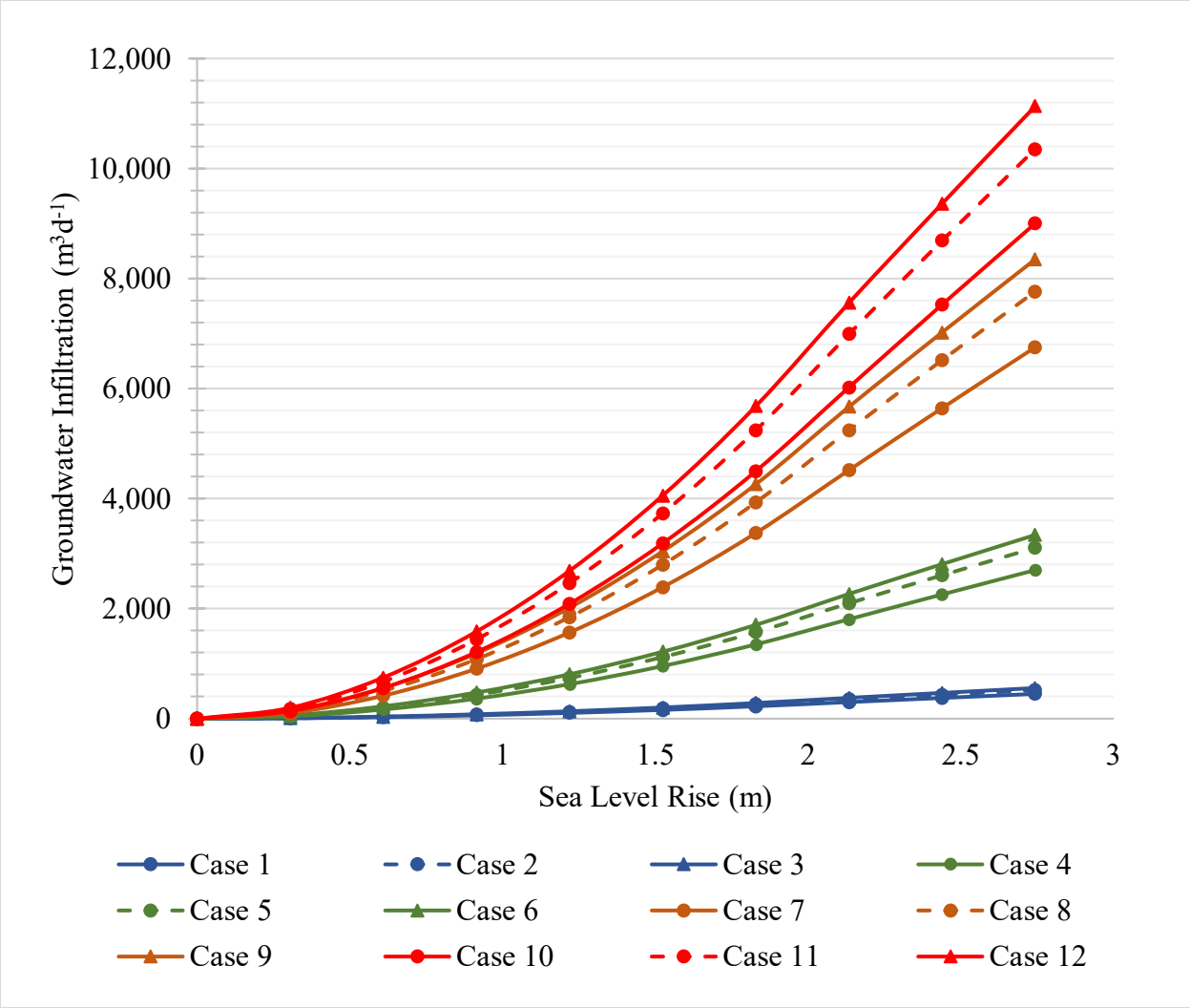

Figure 8. Severity Matrix Cases for SLR Impact on GWI into Sewer Lines Submerged in the Future

3.22 Scenario F-βh: Mathematical Relationship between β and h

The linear method to determining PGWI (Section 3.11) resulted in a trend between defect size and hydraulic head. Therefore, by deriving a relationship between these two variables, a defect size might be estimated with a future hydraulic head. Using the eight DWF days, the mean hydraulic head was calculated for each pipe segment. The mean GWI for each pipe segment ($Q_{Actual,\ Pipe\ Segment}$) was also calculated. The defect sizes were then calibrated with these mean hydraulic heads and $Q_{Actual,\ Pipe\ Segment}$. The resulting defect sizes are plotted against their corresponding hydraulic heads (black squares in Figure 9), and a trendline was fitted (black line

in Figure 9). Since the linear PGWI relationship (equation 7) is a function of pipe size and surrounding soil hydraulic conductivity, there is a different trendline for each combination of pipe size and soil hydraulic conductivity. Equation 10 (h is in units m) presents the polynomial function for pipes with a radius of 12.7 cm and surrounding soil hydraulic conductivity of 4.23E-5 m/s.

$$\beta = 5.1h^2 - 0.73h - 0.0077 \qquad \text{Equation 10}$$

For comparison, Figure 9 includes the β and h curves from the individual calibration of each DWF day. Even though each day meets the DWF criteria, there is a range of relationships between β and h across the DWF days, due to the varying GWI on each DWF day (Table 2).

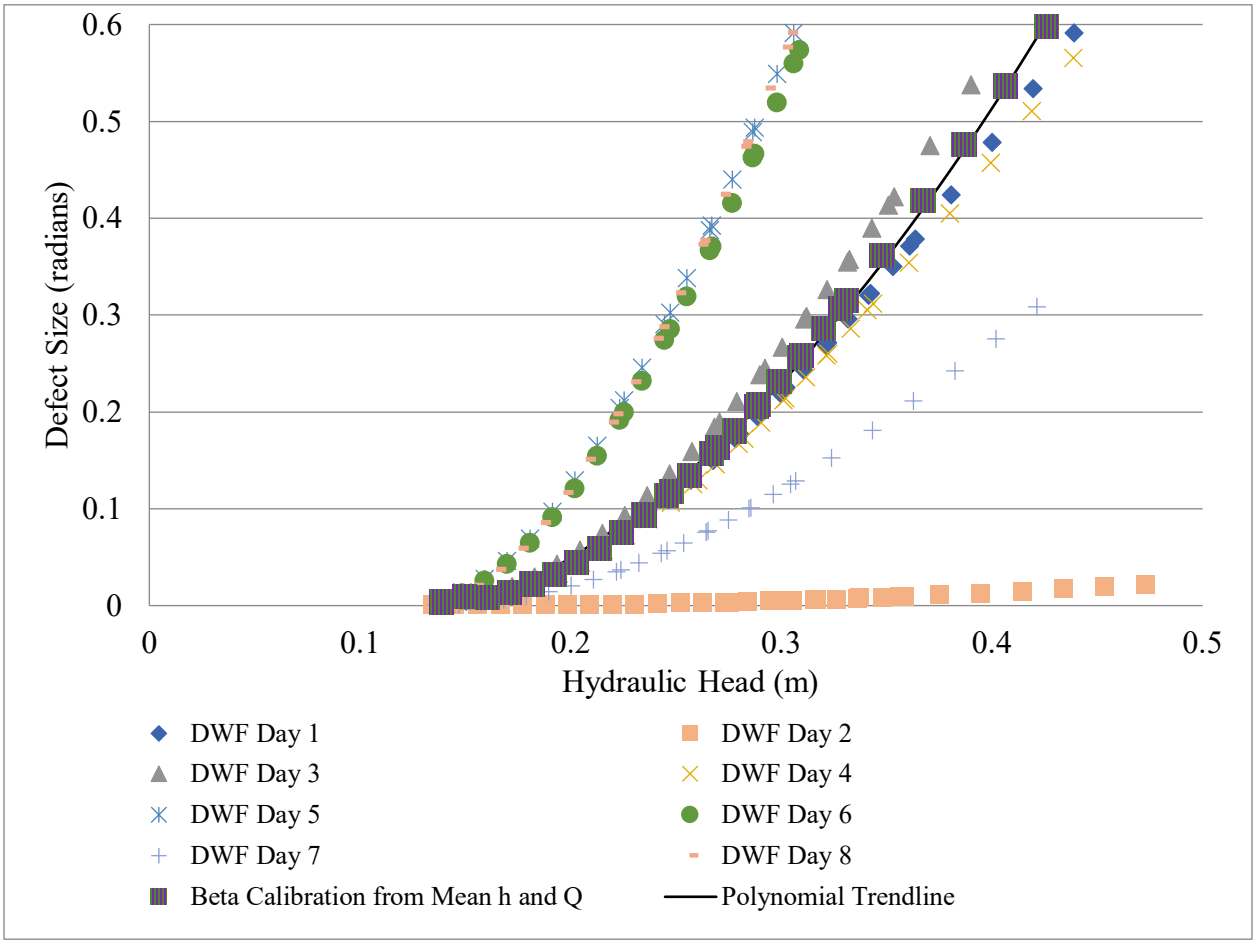

Figure 9. β and h Relationship for Evaluating SLR Impact on GWI

3.23 Scenario F-Eβ: Effective β

As mentioned previously, an effective β offers a way to characterize the system, but it also provides another way to predict future GWI in pipes that will be submerged in the future. The grand mean of the calibrated βs, 0.197 or approximately π/16, was used as the effective β (Figure 6). This value was applied to pipes submerged in the future, and the results are shown as the black squares in Figure 10. To compare results from other effective βs that may exist for other sanitary sewer networks, Figure 10 also includes GWI results from a range of effective βs, from π/10 to π/55.

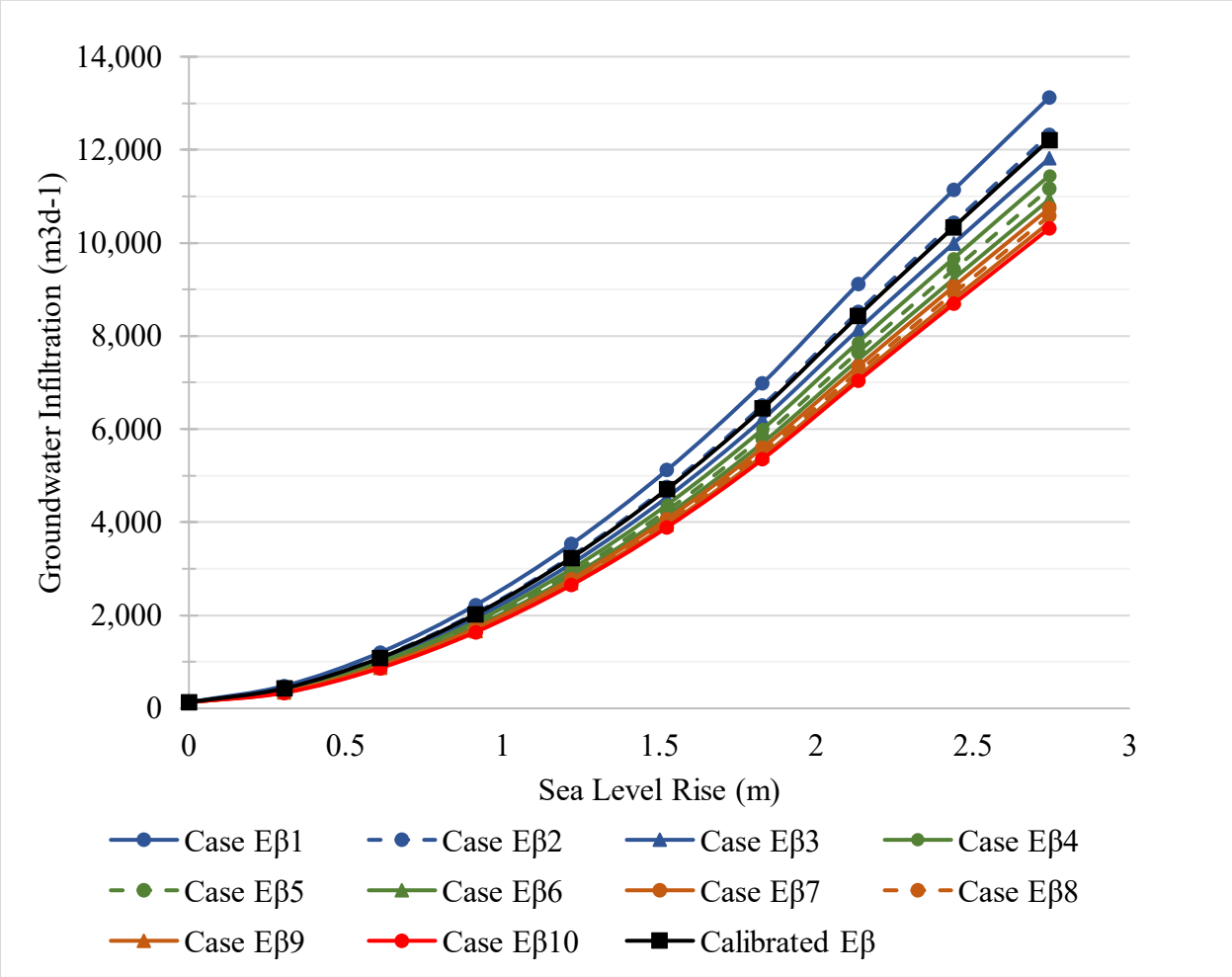

Figure 10. Effects of Varying Effective β for Currently and Eventually Submerged Pipes

Effective β is π/10 for Case Eβ1, π/15 for Case Eβ2, π/20 for Case Eβ3, π/25 for Case Eβ4, π/30 for Case Eβ5, π/35 for Case Eβ6, π/40 for Case Eβ7, π/45 for Case Eβ8, π/50 for Case Eβ9, and π/55 for Case Eβ10.

4.0 DISCUSSION

4.1 Impact of Different PGWI Calculations on Overall Projections

Two methods were used to calculate PGWI: one linear and the other using the 2D model. Compared to the linear relationship, the 2D model method results in a more stable relationship between β and h. For example, as depicted in Figure 11, for DWF Day 1, there is an increasing trend between β and h when using the linear relationship (blue diamonds), while there is little dependency of β on h when using the 2D model (orange squares). The same behavior is observed from the other DWF days. Furthermore, a pipe located at higher groundwater elevations cannot be expected to have a larger crack size; therefore, the 2D model is more accurate for calculating PGWI.

Between the two methods of determining PGWI, however, there is little difference in resulting GWI projections (Figure 12). The percent difference between each of the projections is approximately 4%. However, a benefit of using the 2D model is that an effective β can be ascertained and used for projections of newly submerged pipes (Scenario F-Eβ).

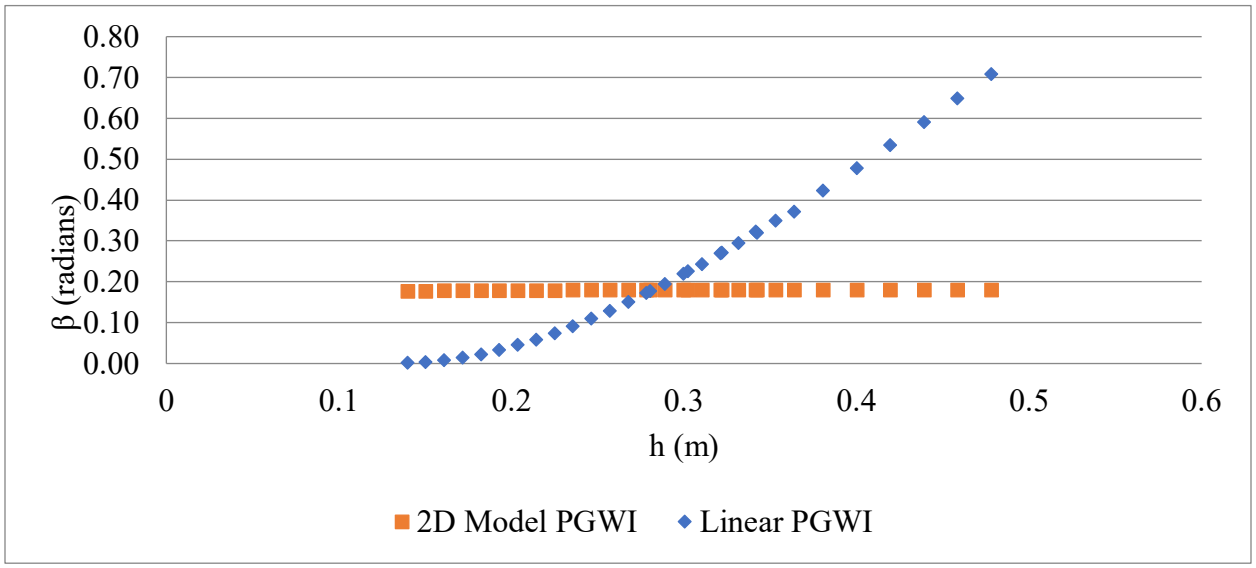

Figure 11. Comparison of β and h Relationship using Different PGWI Calculation Methods

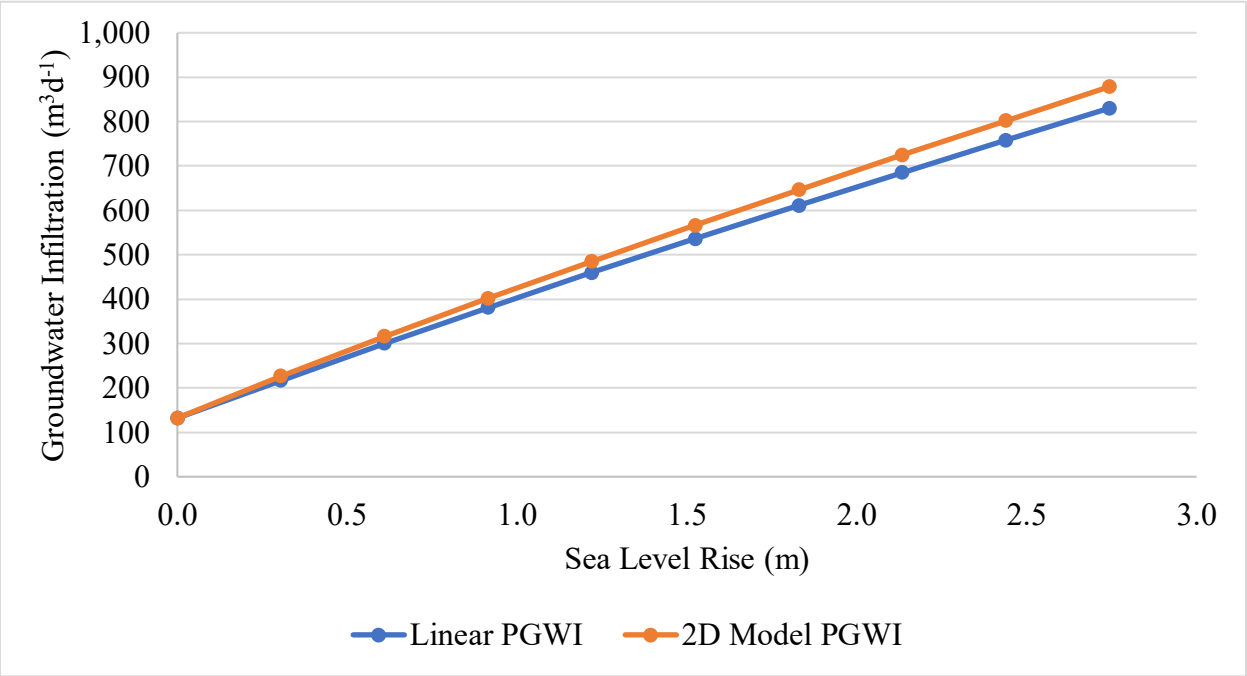

Figure 12. Effect of Different PGWI Relationships on Projections of Groundwater Infiltration

4.2 Unavailable Monitoring Data for Calibration

If monitoring data is not available for model calibration, the severity matrix can still be applied to a sanitary sewer network. Nevertheless, monitoring data is valuable for model calibration, and GWI projections were compared between two situations. Both use the severity matrix (Table 5) for pipes submerged in the future, but for currently submerged pipes, the projections with calibration incorporate calibrated hydraulic conductivities and defect sizes, while the projections without calibration use median hydraulic conductivities from the soil survey and defect sizes from the severity matrix (results from Cases 10, 11, and 12 shown in Figure 13). Overall, among cases 1 to 12, the GWI from uncalibrated projections underestimate GWI by percent differences of 45% to 101%. Both scenarios utilize the severity matrix for eventually submerged pipes, but calibration allowed for more accurate hydraulic conductivities and defect sizes of currently submerged pipes. This demonstrates the added value of flow and rainfall monitoring data for calibration.

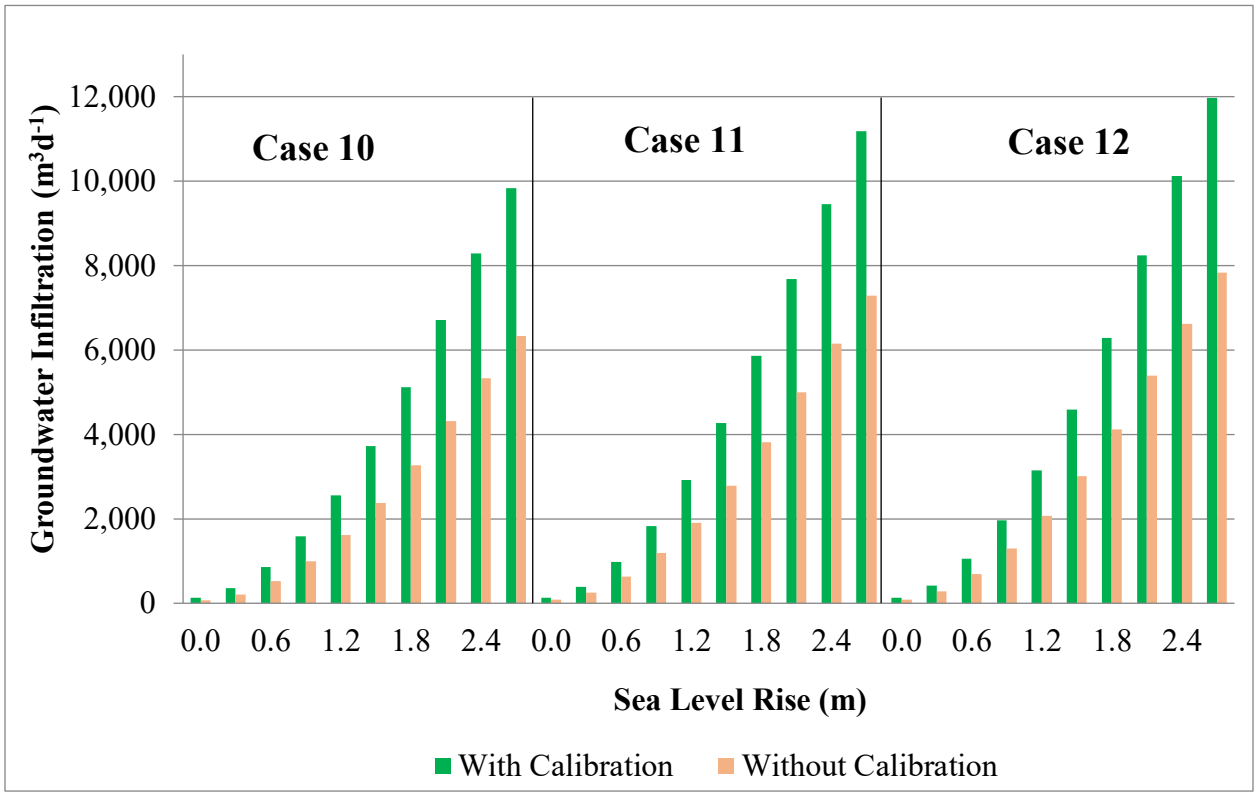

Figure 13. Comparison of Scenarios With and Without Calibration

Note: On the horizontal axis, values of 0 to 2.7 m denote the amount of sea level rise for each case.

4.3 Flowchart for Projecting GWI

With different available ways to project GWI, it seems challenging to decide what technique to use. A flowchart is presented in Figure 14 to assist with determining which method to use, depending on a given situation. If monitoring data is not available, then model calibration is not possible, and the severity matrix (Scenario F-SM) should be used for pipes that are both currently and eventually submerged. If monitoring data is available, then the user should next determine if system knowledge can be applied. This includes identifying areas with worse pipe defects and cracks, which may have been observed during CCTV inspections or smoke testing. If system knowledge can be incorporated into the analysis, then Scenario C-M can be used for currently submerged pipes. For eventually submerged pipes, Scenario F-SM with the severity matrix can be used, with varying severity cases assigned to different sections of the sewer

network based on system knowledge. However, if system knowledge cannot be incorporated, then Scenarios C-M and F-Eβ can be used.

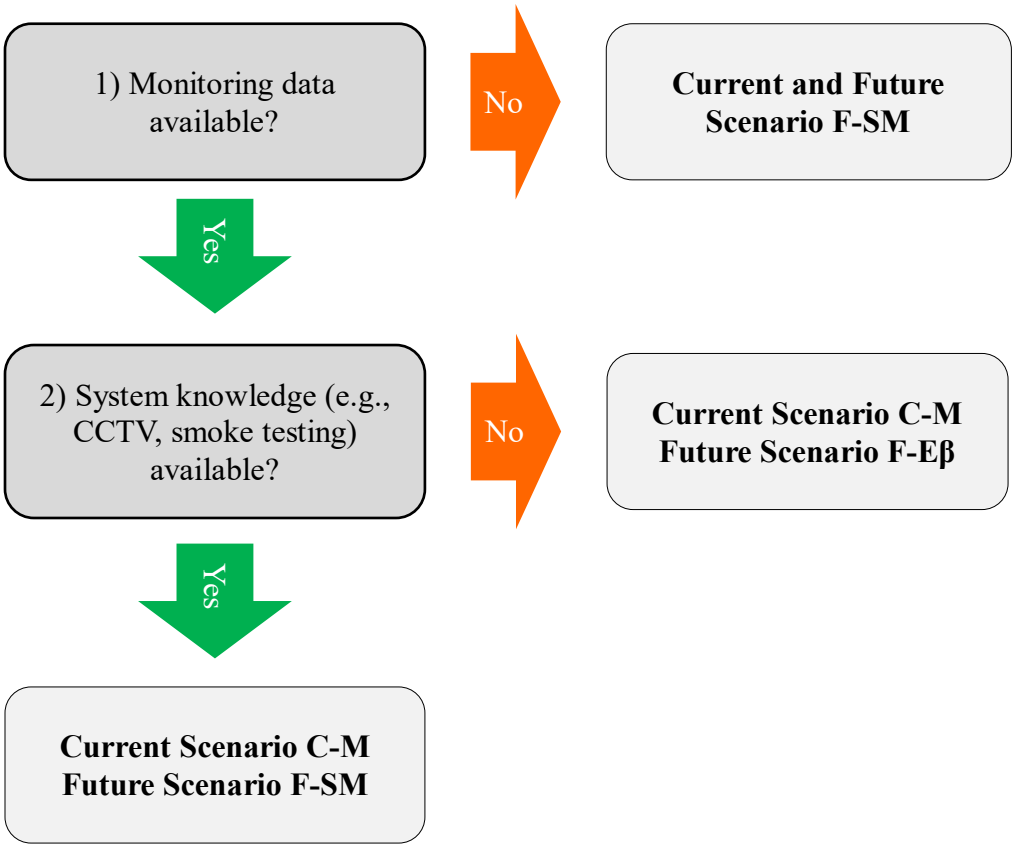

Figure 14. Flowchart for Determining Method to Project GWI

4.4 Statistics of Monitoring Data

Although the selected DWF days met the criteria of little rainfall, there was still variation in the different measurements of GWI (Table 2). While field investigations may provide confirmation or clarification, these require additional resources and costs at the expense of municipalities. Therefore, exploratory data analysis was used to assess data variability.

Scatter plots of the measured levels and velocities at FM-5 were created for easier visualization of the raw data and to show potential graphical correlations between points, orientation of data, bad outliers, and clusters. In the scatter plot of levels measured by FM-5

(orange points in Figure 15), there are reflections of a diurnal pattern, with lower flows prior to 07:00, followed by an increase. There seems to be two streams of data, one between approximately 0.10 and 0.20 m, and another underneath between approximately 0.05 and 0.10 m. This could be caused by tidal influences.

Filtering to view only the DWF days (purple points in Figure 15), there is a similar diurnal trend. However, potential outliers of higher levels can be seen, such as around 02:30, 15:00, and 21:00. Additionally, for any given time, there is a difference of up to roughly 0.05 m in level.

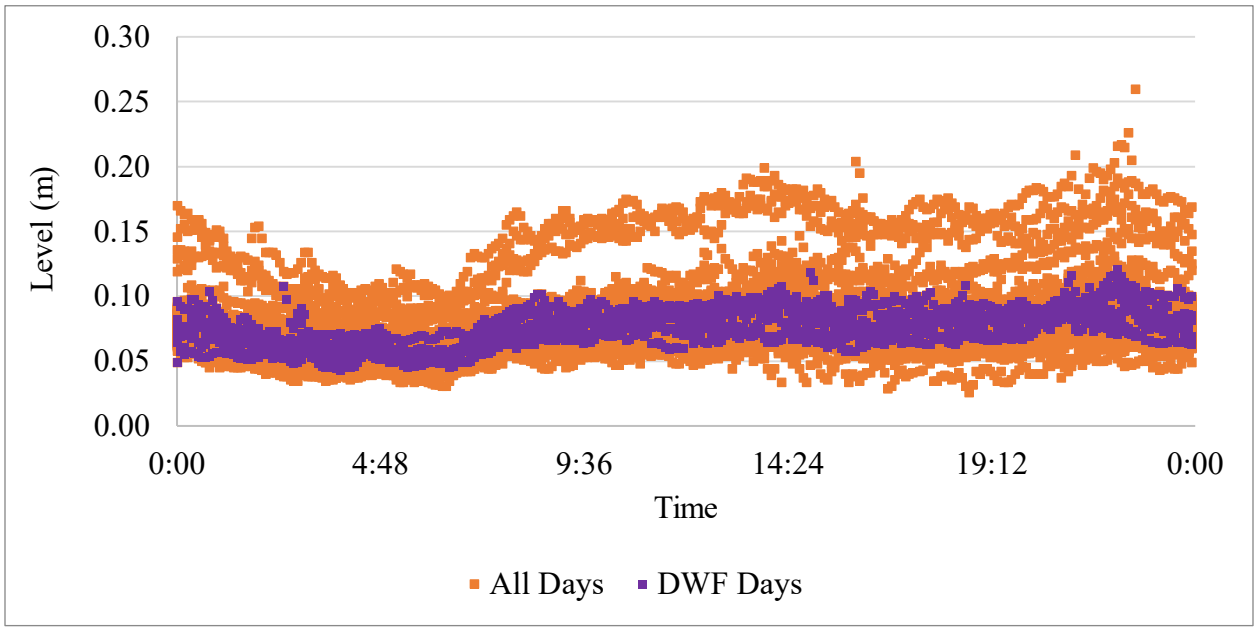

Figure 15. Exploratory Data Analysis of Level Measurements

In the scatter plot for velocity measurements at FM-5 (blue points in Figure 16), most of the data seems to fall below 40,000 m/d, with some scatter between 40,000 and 80,000 m/d. There are also reflections of the diurnal pattern.

Filtering to include just the dry weather flow days allows clearer patterns to be seen, as shown by the green triangles in Figure 16. FM-5 data distinctly shows a fall in velocity between midnight and 07:00, with more stable measurements throughout the day. There are potential

outliers, with some from 0:00 to 02:00, and others scattered throughout the rest of the day. For any given time, there is a difference of up to roughly 10,000 m/d in the velocity measurements.

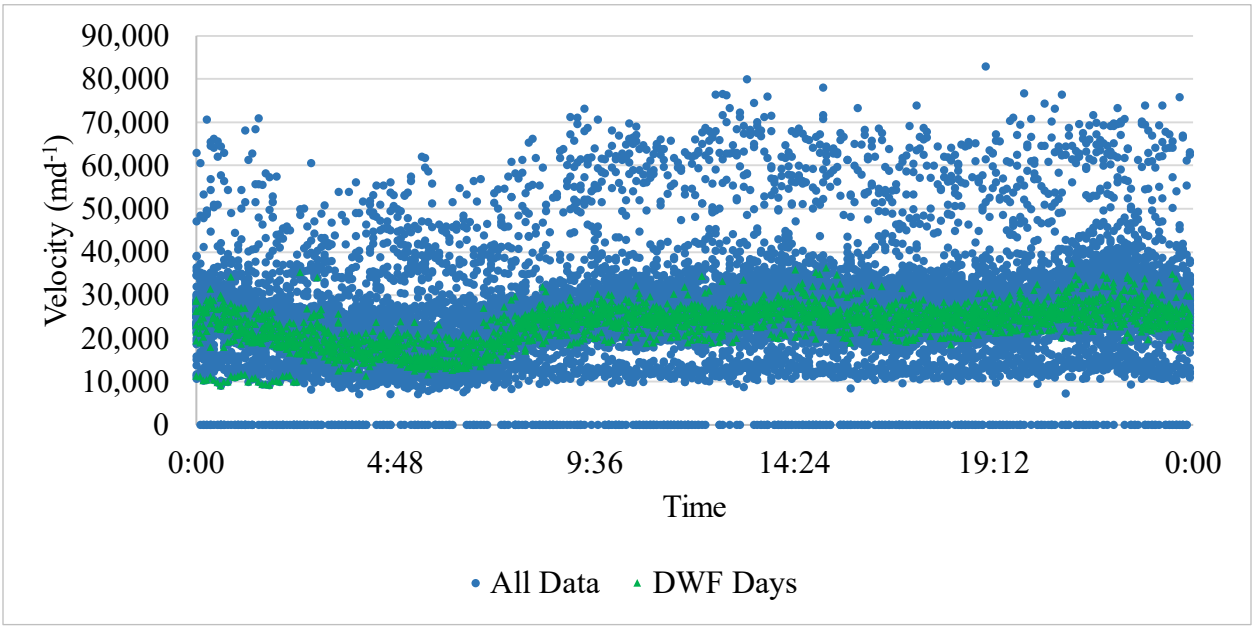

Figure 16. Exploratory Data Analysis of Velocity Measurements

To further demonstrate the variability among the DWF days, Figure 17 plots the daily flow for each DWF day. While the general diurnal trend is visible, there are a few prominent peaks, especially for DWF Days 2 and 3, and dips, such as for DWF Days 2, 5, 6, and 7. Tidal influences and various changes in residential or commercial activities surrounding FM-5 could account for the potential outliers. Therefore, additional information about effects on the study area could further refine analysis and model calibration.

Additionally, other system structures such as lateral lines or pipe joints play a role in non-wastewater contribution to the sanitary sewer flow. Lateral lines are more susceptible to damage, and cracks formed at the connections between lateral and main lines can create pathways for more GWI. These are not usually monitored directly, but there may be ways to incorporate them into GWI projections. For example, a percentage of lateral lines or pipe joints

could be applied based on a literature review, conditional assessment, or CCTV results. These could be assigned a different severity matrix case or effective β.

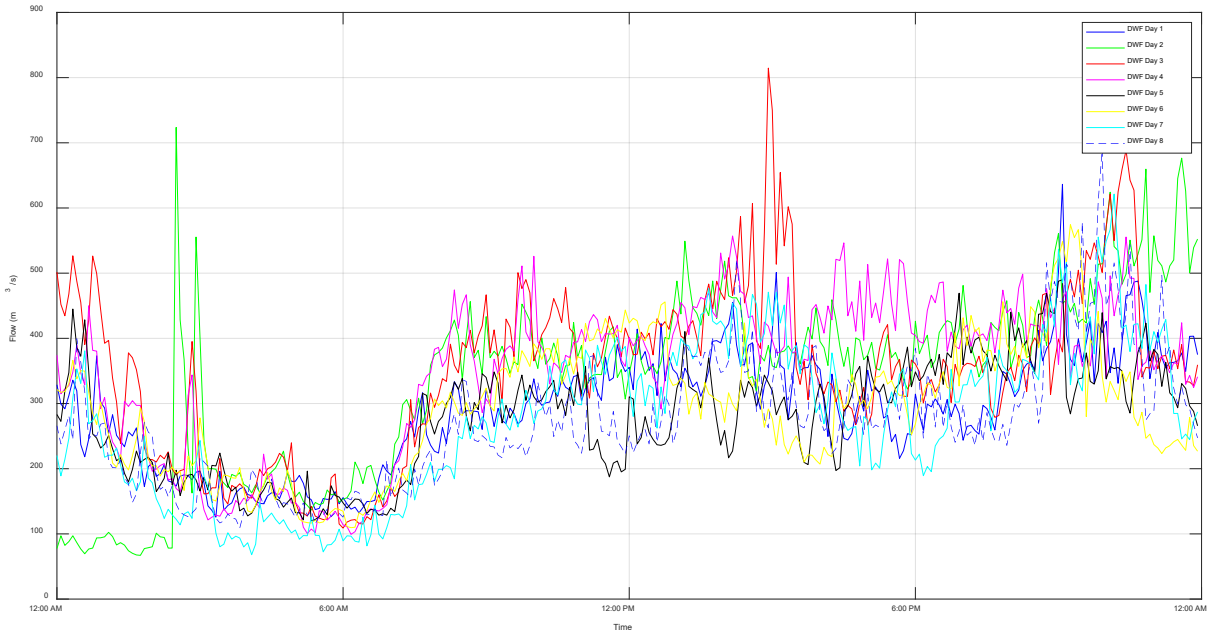

Figure 17. Hydrograph for all DWF Days

5.0 CONCLUSIONS

As sea level increases, more pipes will become submerged by the groundwater table and potentially vulnerable to GWI. To project GWI and prioritize areas for improvements, various models have been developed, but municipalities, planners, and engineers seek both a reliable and user-friendly method. This was achieved in the procedure of calibrating a 2D GWI model with flow monitoring data and applying various SLR scenarios to project future GWI. Easily accessible software from the U.S. EPA and Microsoft Office were used.

Flow and rainfall monitoring data from a coastal sanitary sewer network were evaluated by SSOAP Toolbox, and a flow meter was selected for testing GWI projections. Because the recorded measurements are sums of the upstream lines, the network was segmented into 3-m lines, and GWI for each segment was calculated based on a proportion with PGWI. Two

methods were investigated for calculating PGWI for individual pipe segments, one using a linear relationship, and the other using a 2D GWI model.

Other data were also obtained from the sanitary sewer system GIS database, the USDA NRCS, and USGS. These data inputs, along with the calculated GWI per segment, were used to calibrate the 2D GWI model.

There were two separate applications of the model: one for currently submerged pipes and the other for eventually submerged pipes. In the first, the model was calibrated for β using the two different methods of calculating PWGI, resulting in Scenarios C-L and C-M. Afterwards, the hydraulic heads of the calibrated model were adjusted depending on the amount of SLR. The resulting projections from each PGWI method were only about 4% percent different; however, the 2D GWI model allows for calculating an effective β that can be used in projections of newly submerged pipes.

In the second application of the model, three methods were tested for projecting GWI of pipes submerged in the future:

1. Scenario F-SM: A severity matrix was set up with cases of varying degrees of pipe defects and lengths of pipes affected by GWI. The cases can be translated to represent areas with better or worse conditions, based on system knowledge.
2. Scenario F-βh: A mathematical expression between β and h was determined using GWI data from currently submerged pipes. This was used to determine β for newly submerged pipes as sea level rises and h changes, but this is not a recommended method because the mathematical expression shows an increasing polynomial relationship between β and h.
3. Scenario F-Eβ: The calculation of PGWI using the 2D GWI model resulted in an effective β that could be used to measure the overall porosity of the system.

A flow chart was developed to tie together the different methods depending on data or system knowledge that is available (Figure 14). Each of the procedures provide GWI projections that can be relatively easy to obtain, quantitatively defended, and effectively used to mitigate the effects of SLR and GWI on sanitary sewers.

6.0 REFERENCES

[1] R. Etkins and E. S. Epstein, "The Rise of Global Mean Sea Level Change as an Indication of Climate Change," Science, vol. 215, no. 4530, pp. 287-289, 1982.

[2] R. J. Nicholls and A. Cazenave, "Sea-Level Rise and Its Impact on Coastal Zones," Science, vol. 328, no. 5985, pp. 1517-1520, 2010.

[3] NOAA, "Global and Regional Sea Level Rise Scenarios for the United States," NOAA, Silver Spring, 2017.

[4] R. S. Nerem, B. D. Beckley, J. T. Fasullo, B. D. Hamlington, D. Masters and G. Mitchum, "Climate-change–driven accelerated sea-level rise detected in the altimeter era," Proceedings of the National Academy of Sciences of the United States of America, vol. 115, no. 9, pp. 2022-2025, 2018.

[5] K. Rotzoll and C. H. Fletcher, "Assessment of Groundwater Inundation as Consequence of Sea-Level Rise," Nature Climate Change, vol. 3, pp. 477-481, 2013.

[6] S. Habel, C. H. Fletcher, K. Rotzoll and A. I. El-Kadi, "Development of a Model to Simulate Groundwater Inundation Induced by Sea-Level Rise and High Tides in Honolulu, Hawaii," Water Research, vol. 114, pp. 122-134, 2017.

[7] J. P. a. S. P. G. Masterson, "Effects of Sea-Level Rise on Ground Water Flow in a Coastal Aquifer System," Ground Water, vol. 45, no. 2, pp. 209-217, 2007.

[8] J. P. Masterson, "Simulated Interaction Between Freshwater and Saltwater and Effects of Ground-Water Pumping and Sea-Level Change, Lower Cape Cod Aquifer System, Massachusetts, Scientific Investigations Report 2004-5014," U.S. Geological Survey, Denver, 2004.

[9] G. E. v. B. a. P. B. d. L. P. Oude Essink, "Effects of climate change on coastal groundwater systems: A modeling study in the Netherlands," Water Resources Research, vol. 46, no. W00F04, pp. 1-16, 2010.

[10] D. M. J. R. M. J. R. S. B. J. S. a. M. A. R. Bjerklie, "Preliminary investigation of the effects of sea-level rise on groundwater levels in New Haven, Connecticut, U.S. Geological Survey Open-File Report," U.S. Geological Survey, Reston, 2012.

[11] A. K. M. S. S. D. J. M. a. M. T. G. Manda, "Relative role and extent of marine and groundwater inundation on a dune-dominated barrier island under sea-level rise scenarios," Hydrological Processes, vol. 29, no. 8, pp. 1894-1904, 2014.

[12] J. P. M. N. F. E. R. T. D. B. G. B. T. G. a. N. G. P. Masterson, Effects of sea-level rise on barrier island groundwater system dynamics - ecohydrological implications, vol. 7, no. 3, pp. 1064-1071, Ecohydrology.

[13] H. C. Z. a. D. S. Cooper, "Incorporating Uncertainty of Groundwater Modeling in Sea-Level Rise Assessment: a Case Study in South Florida," Climate Change, vol. 129, no. 1-2, pp. 281-294, 2015.

[14] D. A. T. D. M. J. P. M. a. M. N. a. F. Walter, "Potential effects of sea-level rise on the depth to saturated sediments of the Sagamore and Monomoy flow lenses on Cape Cod,

Massachusetts, Scientific Investigations Report 2016-5058," U.S. Geological Survey, Reston, 2016.
[15] D. DeSilva, S. Burn, G. Tjandraatmadja, M. Moglia, P. Davis, L. Wolf, I. Held, J. Vollertsen, W. Williams and L. Hafskjold, "Sustainable Management of Leakage from Wastewater Pipelines," Water Science & Technology, vol. 52, no. 12, pp. 189-198, 2005.
[16] H. Wittenberg and H. Aksoy, "Groundwater Intrusion into Leaky Sewer System," Water Science & Technology, vol. 62.1, pp. 92-98, 2010.
[17] C. Karpf, T. Franz and P. Krebs, "Fractionation of Infiltration and Inflow (I/I) Components in Urban Sewer Systems with Regression Analysis," Novatech, pp. 1227-1234, 2007.
[18] National Small Flows Clearinghouse, "Pipeline, Small Community Wastewater Issues Explained to the Public," National Small Flows Clearinghouse, West Virginia, 1999.
[19] The Corporation of the City of Vaughan, "Inflow and Infiltration Reduction Program," The Corporation of the City of Vaughan, 2018. [Online]. Available: https://www.vaughan.ca/services/residential/wastewater/Pages/Inflow-and-Infiltration-Reduction-Program.aspx. [Accessed 9 July 2018].
[20] L. Wolf, J. Klinger, I. Held and H. Hotzl, "Integrating groundwater into urban water management," Water Science & Technology, vol. 54, no. 6-7, pp. 395-403, 2006.
[21] G. Dirckx, S. Van Daele and N. Hellinck, "Groundwater Infiltration Potential (GWIP) as an Aid to Determining the Cause of Dilution of Waste Water," Journal of Hydrology, vol. 542, pp. 474-486, 2016.
[22] C. Karpf, S. Hoeft, C. Scheffer, L. Fuchs and P. Krebs, "Groundwater Infiltration, Surface Water Inflow and Sewerage Exfiltration Considering Hydrodynamic Conditions in Sewer Systems," Water Science & Technology, vol. 63, no. 9, pp. 1841-1848, 2011.
[23] S. Thorndahl, J. D. Balling and U. B. B. Larsen, "Analysis and Integrated Modelling of Groundwater Infiltration to Sewer Networks," Hydrological Processes, vol. 30, pp. 3228-3238, 2016.
[24] C. Karpf and P. Krebs, "Quantification of Groundwater Infiltration and Surface Water Inflows in Urban Sewer Networks Based on a Multiple Model Approach," Water Research, vol. 45, pp. 3129-3136, 2011.
[25] C. Karpf and P. Krebs, "Modelling of Groundwater Infiltration into Sewer Systems," Urban Water Journal, vol. 10, no. 4, pp. 221-229, 2013.
[26] S. Guo, T. Zhang, Y. Zhang and D. Z. Zhu, "An approximate solution for two-dimensional groundwater infiltration in sewer systems," Water Science & Technology, pp. 347-352, 2013.
[27] Teledyne Technologies Incorporated, "2150 Area Velocity Module," 2013. [Online]. Available: https://www.teledyneisco.com/en-us/waterandwastewater/Flow%20Meter%20Documents/Brochures/2100%20Series%20Flow%20Modules%20Brochure.pdf.

[28] P. Staufer, A. Scheidegger and J. Rieckermann, "Assessing the Performance of Sewer Rehabilitation on the Reduction of Infiltration and Inflow," Water Research, vol. 46, pp. 5185-5196, 2013.
[29] U.S. EPA, "Computer Tools for Sanitary Sewer System Capacity Analysis and Planning," U.S. EPA, Washington, D.C., 2007.
[30] J. P. Davies, B. A. Clarke, J. T. Whiter and R. J. Cunningham, "Factors influencing the structural deterioration and collapse of rigid sewer pipes," Urban Water, vol. 3, pp. 73-89, 2001.
[31] Z. Tan, "Nonlinear Finite Element Study of Deteriorated Rigid Sewers Including the Influence of Erosion Voids," Department of Civil Engineering, Queen's University at Kingston, Ontario, 2007.
[32] J. F. Knott, J. M. Jacobs, J. S. Daniel and P. and Kirshen, "Modeling the effects of sea-level rise on groundwater levels in coastal New Hampshire," [Online]. Available: https://www.unh.edu/erg/sites/www.unh.edu.erg/files/modeling_the_effects_of_sea-level_rise_on_groundwater_levels_in_coastal_nh.pdf. [Accessed 17 July 2018].
[33] A. P. B. V. B. D. C. M. C. J. H. R. H. K. K. R. M. J. O. A. S. a. J. W. Parris, "Global Sea Level Rise Scenarios for the US National Climate Assesment, NOAA Technical Report OAR CPO-1," National Oceanic and Atmospheric Administration, Silver Spring, 2012.
[34] U.S. EPA, "Report to Congress, Impacts and Controls of CSOs and SSOs," August 2004. [Online]. Available: https://www.epa.gov/sites/production/files/2015-10/documents/csossortc2004_full.pdf. [Accessed 10 June 2018].
[35] U.S. EPA, "CWNS 2000 Report to Congress," 2000. [Online]. Available: https://www.epa.gov/cwns/cwns-2000-report-congress. [Accessed 2018].
[36] R. Collins and J. Boxall, "Influence of Ground Conditions on Intrusion Flows through Apertures in Distribution Pipes," Journal of Hydraulic Engineering, vol. 139, no. 10, pp. 1052-1061, 2013.
[37] O. Kracht, M. Gresch, J. deBenedittis, V. Prigiobbe and W. Gujer, "Stable Isotopes of Water as Natural Tracer for Infiltration into Urban Sewer Systems," Geophysical Research Abstracts, vol. 8, no. 07852, 2003.
[38] O. Kracht and W. Gujer, "Quantification of Infiltration into Sewers Based on Time Series of Pollutant Loads," Water Science & Technology, vol. 52, no. 3, pp. 209-218, 2005.
[39] M. El Tani, "Circular Tunnel in a Semi-Infinite Aquifer," Tunnelling and Underground Space Technology, vol. 18, no. 1, pp. 49-55, 2003.
[40] D. Kolymbas and P. Wagner, "Groundwater Ingress into Tunnel - The Exact Analytical Solution," Tunnelling and Underground Space Technology, vol. 22, pp. 23-27, 2007.
[41] S. Lei, "An Analytical Solution for Steady Flow into a Tunnel," Ground Water, vol. 37, no. 1, pp. 23-26t, 1999.
[42] K. H. Park, A. Owatsiriwong and J. G. Lee, "Analytical Solution for Steady-State Groundwater Inflow into a Drained Circular Tunnel in a Semi-Infinite Aquifer: a Revisit," Tunnelling and Underground Space Technology, vol. 23, no. 2, pp. 206-209, 2008.

[43] S. Guo, Y. Yang and Y. Zhang, "An approximate model on three-dimensional groundwater infiltration in sewer systems," Water Science & Technology, vol. 77, no. 11, 2016.
[44] K. Weeman and P. Lynch, "Global Climate Change," National Aeronautics and Space Administration Jet Propulsion Laboratory, 13 February 2018. [Online]. Available: https://climate.nasa.gov/news/2680/new-study-finds-sea-level-rise-accelerating/. [Accessed 9 July 2018].